

## Clinical Article

# Assessment of the Intracranial Stents Patency and Re-Stenosis by 16-Slice CT Angiography with Optimized Sharp Kernel : Preliminary Study

Ki Seok Choo, M.D.,<sup>1</sup> Tae Hong Lee, M.D.,<sup>2</sup> Chang Hwa Choi, M.D.,<sup>3</sup> Kyung Pil Park, M.D.,<sup>4</sup> Chang Won Kim, M.D.,<sup>2</sup> Suk Kim, M.D.<sup>2</sup>

Departments of Diagnostic Radiology,<sup>1</sup> Neurology,<sup>4</sup> Pusan National University Yangsan Hospital, Pusan National University School of Medicine, Busan, Korea

Departments of Diagnostic Radiology,<sup>2</sup> Neurosurgery,<sup>3</sup> Pusan National University Hospital, Pusan National University School of Medicine, Busan, Korea

**Objective :** Our retrospective study aimed to determine whether 16-slice computerized tomography (CT) angiography optimized sharp kernel is suitable for the evaluation of visibility, luminal patency and re-stenosis of intracranial stents in comparison with conventional angiography.

**Methods :** Fifteen patients with symptomatic intracranial stenotic lesions underwent balloon expandable stent deployment of these lesions (10 middle cerebral arteries, 2 intracranial vertebral arteries, and 3 intracranial internal carotid arteries). CT angiography follow-up ranged from 6 to 15 months (mean follow-up, 8 months) after implantation of intracranial stents and conventional angiography was confirmed within 2 days. Curved multiplanar reformations with maximal intensity projection (MIP) with optimal window settings for assessment of lumen of intracranial stents were evaluated for visible lumen diameter, stent patency (contrast distal to the stent as an indirect sign), and re-stenosis by two experienced radiologists who blinded to the reports from the conventional angiography.

**Results :** All of stents deployed into symptomatic stenotic lesions. All stents were classified as patent and no re-stenosis, which was correlated with results of conventional angiography. Parts of the stent lumen could be visualized in all cases. On average, 57% of the stent lumen diameter was visible using optimized sharp kernel. Significant improvement of lumen visualization (22%,  $p < 0.01$ ) was observed using the optimized sharp kernel compared with the standard sharp kernel. Inter-observer agreements on the measurement of lumen diameter and density were judged as good, respectively ( $p < 0.05$ ).

**Conclusion :** Sixteen-slice CT using the optimized sharp kernel may provide a useful information for evaluation of lumen diameter patency, and re-stenosis of intracranial stents.

**KEY WORDS :** Intracranial atherosclerosis · Stents · Multislice CT · CT angiography · Cerebral angiography.

## INTRODUCTION

In coronary, peripheral, and extracranial cerebral circulation, stenting has been shown to increase the safety and efficacy of balloon angioplasty for the treatment of arterial lesions<sup>2,7,21</sup>. More recently, elective stenting of atherosclerotic intracranial artery stenosis as an alternative treatment modality has become possible due to the introduction of the newer, more flexible coronary stents<sup>8-10,17</sup>. One major pro-

blem of angioplasty with stenting, however, is the occurrence of in-stent restenoses, which may be caused by stent thrombosis, neointimal growth or inflammation of the vessel wall with proliferation of the extracellular matrix<sup>6</sup>. The method of choice for the detection of restenoses within stented vessel segments is intra-arterial catheter angiography<sup>18</sup>. This invasive method, however, has the disadvantage of a moderate to high cost and unanticipated, though rare, serious complications<sup>4,19,20</sup>. Therefore, a non-invasive alternative method for assessment of the intracranial stented vessel would be highly desirable<sup>12</sup>. The recent introduction of 16-slice Multislice CT (MSCT) systems has further improved in spatial and temporal resolution.

*In vitro* studies, the minimum diameter of stents for reliable differentiation between in-stent restenoses and vessel

• Received : February 25, 2009 • Accepted : April 26, 2009

• Address for reprints : Tae Hong Lee, M.D.  
Department of Diagnostic Radiology, Pusan National University  
Hospital, Pusan National University School of Medicine, Ami-dong 10-1-  
ga, Seo-gu, Busan 602-739, Korea  
Tel : +82-51-240-7354, Fax : +82-51-244-7534  
E-mail : drcello@pusan.ac.kr

occlusion using CT was 4.0 mm<sup>18)</sup> and 16-slice MSCT with a dedicated reconstruction kernel offered improved visualization of coronary artery stents and facilitated delineation of in-stent stenosis<sup>13)</sup>. The purpose of the present study was to assess lumen visibility, patency and re-stenosis of intracranial stents using 16-slice MSCT with an optimized reconstruction kernel *in vivo*.

**MATERIALS AND METHODS**

**Patients**

The study population included 15 patients (13 Male, 2 Female, average age 62 years) who had been treated with intracranial stents implantation between January and December 2004. A total 15 stents of single type were evaluated in 15 patients. Ten stents were located in the middle cerebral arteries, 2 stents in the intracranial vertebral arteries and 3 stents in the pterocavernous portion of internal carotid artery. Written informed consent was obtained from all participants.

**Computed tomography protocol**

Sixteen-slice CT images were acquired on a sensation 16 (Siemens Medical Solutions, Forchheim, Germany) at 6.2 ±1.3 months after intracranial stents placement in all patients with a detector collimation of 16×0.75 mm and a Table 1 feed of 2.8 mm per rotation. Rotation time was 420 milliseconds, tube current 370 mAs, and tube voltage 120 Kvp. The field of view was 100 mm with a 512×512 matrix. For contrast enhancement, 120 mL of contrast media (Ultravist, Shering, Germany) were administered intravenously at a flow rate of 4 mm/sec. Scan delay was determined with an automatic bolus tracking system. One round region of interest was placed on common carotid artery. A threshold level of 100 HU was set for starting the scan. Axial images with an effective slice thickness of 0.75 mm were created with a 0.8-mm image increment using the optimized sharp kernel (H60f) and the standard sharp kernel (H31f). Curved multiplanar reformations with thin (0.8 mm) maximal intensity projection (MIP) with optimal window settings for assessment of lumen of intracranial stents were created on workstation.

**Evaluation of lumen visibility, patency and in stent re-stenosis**

Stent lumen visibility was interactively evaluated by two radiologists independently who were unaware of the reports from the catheter angiographies performed within 2 days after CT scan and clinical information about patients. The diameter of proximal vessel lumen to the stent and stent lumen were measured semi-automatically on largely displayed work station (Wizard, Siemens Medical Solutions, Forch-

heim, Germany) and the percentage of the vessel diameter with each optimized sharp kernel (H60f) and the standard sharp kernel (H31f). The region of interest (ROI) included 5 pixels and was placed in the center of the visible stent lumen without inclusion of the stent struts and center of the vessel lumen proximal and distal to stent with optimized sharp kernel (H60f). Three densities in stent lumen (proximal, middle and distal in lumen) were averaged and two ones in vessel (proximal and distal to stent) were also done. Differences between the measurements of visible lumen diameter on CT angiography with the standard sharp kernel (H31f) and optimized sharp kernel (H60f) were statistically evaluated using the paired t-test. Inter-observer agreement on the measurement of visible lumen diameter and density was also evaluated using the paired t-test.

Stent patency and in stent re-stenosis were assessed with optimized sharp kernel (H60f) by two radiologists with consensus. Vessel contrast distal to the stent was recorded for each stent as an indirect sign of stent patency, and detection of in-stent restenosis was based on visual assessment.

**RESULTS**

All CT examinations were completed without adverse events following contrast media application and without other complications and the image quality of the stented vessels were fair to good. Using optimized sharp kernel (H60f), the average visible lumen diameter ranged from 48% to 73% (average : 60%) in observer 1, 45% to 73% (average : 57%) in observer 2, respectively, and using standard sharp kernel (H31f), the average visible lumen diameter ranged from 24% to 51% (average : 35%) in observer 1, 25% to 52% (average : 35%) in observer 2, respectively. Using optimized sharp kernel (H60f) for reconstruction, improvements in lumen visibility were recorded (average 25%, 22% in observer 1, 2 respectively, *p*<0.01) (Fig. 1, 2, 3). Averaged stent lumen densities and vessel lumen densities were 310, 225 HU and 318, 212 HU in observer 1, observer 2, respectively. Density of stent lumen was statistically significant less than that of vessel lumen (*p*<0.05). Inter-observer agreements on the measurement of

**Table 1.** Average lumen visibility with different kernels according to the diameter of the stent

Stent Diameter (mm)	Average Lumen Visibility with Different Kernels (% observer 1/observer 2)	
	H60f	H31f
2.5	53.6/51.1	31.5/30.3
3.5	68.5/68.7	48.3/49.5
4	71.3/70.4	47.8/42.9

H60f : optimized sharp kernel, H31f : standard sharp kernel

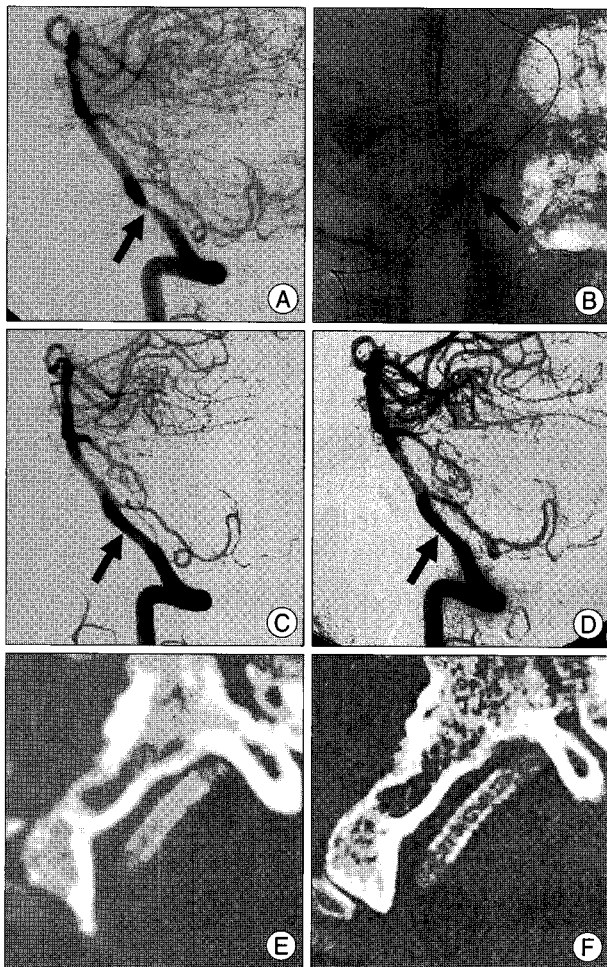


**Fig. 1.** A 55-year-old male presented with dysarthria, dizziness, and gait disturbance. A : Lateral view of the right VA angiogram shows focal severe stenosis (arrow, about 80%) proximal to the PICA (Posterior Inferior Cerebellar Artery) origin of right VA. B : Anteroposterior radiographs show the stent (arrow) during deployment in the stenotic segment of right VA. The used stent is a 4.0/16 mm-sized, balloon-mounted coronary stent (Flexmaster, JoMed, Rangendingen, Germany). C : Immediate postprocedural lateral view of the right VA angiogram reveals nearly normalized diameter of the diseased vessel (arrow). D : After 6 months, follow-up lateral angiogram shows no in-stent restenosis. E : Computed tomography angiography with 16 MSCT is performed at 24 hours after follow-up angiography. Curved axial multiplanar reconstruction with standard sharp kernel (H31f) shows about 47% lumen visibility on the right intracranial vertebral artery. F : Curved axial multiplanar reconstruction with optimized sharp kernel (H60f) shows about 71% lumen visibility on the right intracranial vertebral artery.

lumen diameter and density were judged as good ( $p < 0.05$ ).

In all cases, the vessel part distal to the stent had the contrast as an indirect sign of stent patency and evaluation of in-stent restenosis was based on visual estimation. All cases were confirmed by conventional angiography.

## DISCUSSION

Compared with balloon angioplasty, the advantages of stent-assisted angioplasty include exclusion of the plaque

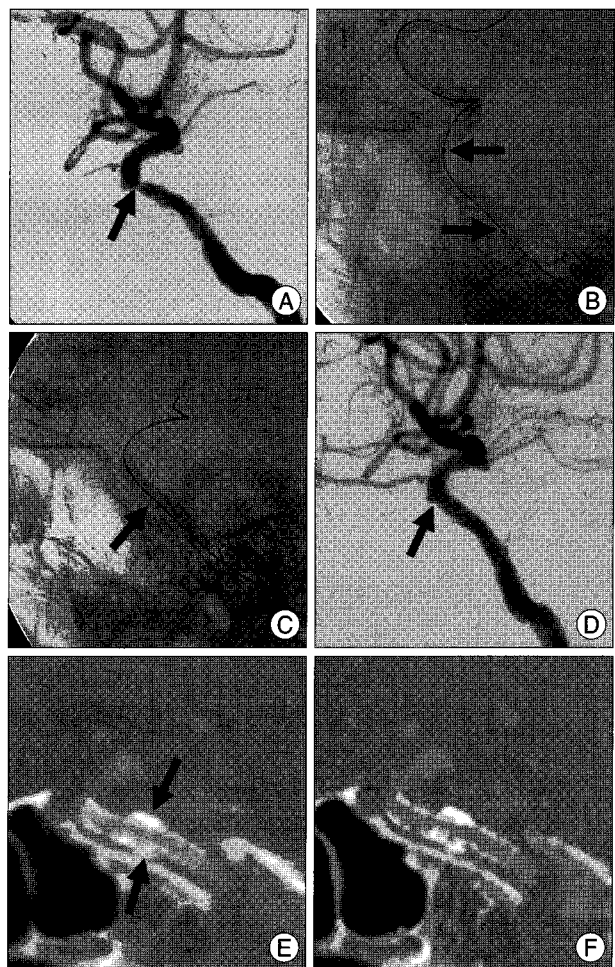


**Fig. 2.** A 63-year-old male presented with recurrent TIA of left hemiparesis. A : Lateral view of the right internal carotid artery (ICA) angiogram shows focal severe stenosis (arrow, about 80%) of the right cavernous ICA correlating with recurrent TIA symptoms. B : A stent (arrow) is positioned at the site of the lesion on the lateral view of the right ICA angiogram. The used stent is a 3.5/19 mm-sized coronary stent (Flexmaster, JoMed). C : Lateral radiographs show the stent (arrow) during deployment in the stenotic segment of right cavernous ICA. D : After 5 months, follow-up lateral angiogram shows no in-stent restenosis. E : Computed tomography angiography with 16 MSCT is performed at 24 hours after follow-up angiography. Curved sagittal multiplanar reconstruction with optimized sharp kernel (H60f) shows about 51% lumen visibility on the petrocavernous portion of right ICA. F : Curved sagittal multiplanar reconstruction with optimized sharp kernel (H60f) shows about 69% lumen visibility on the petrocavernous portion of right ICA.

and regions of dissection from the vessel lumen, prevention of vessel recoil and rupture, and improvement of immediate and long-term patency of the treated lesion<sup>3,9,10</sup>. In the past, the use of stent placement for intracranial arterial stenosis was limited by the inability of the stent catheter to track into the stenotic portion. Recently, however, stenting of intracranial stenosis has been possible with marked advancement in stent technology; the technical feasibility and clinically favorable short- and long-term outcomes of stent placement have been reported in patients with symptomatic intra-

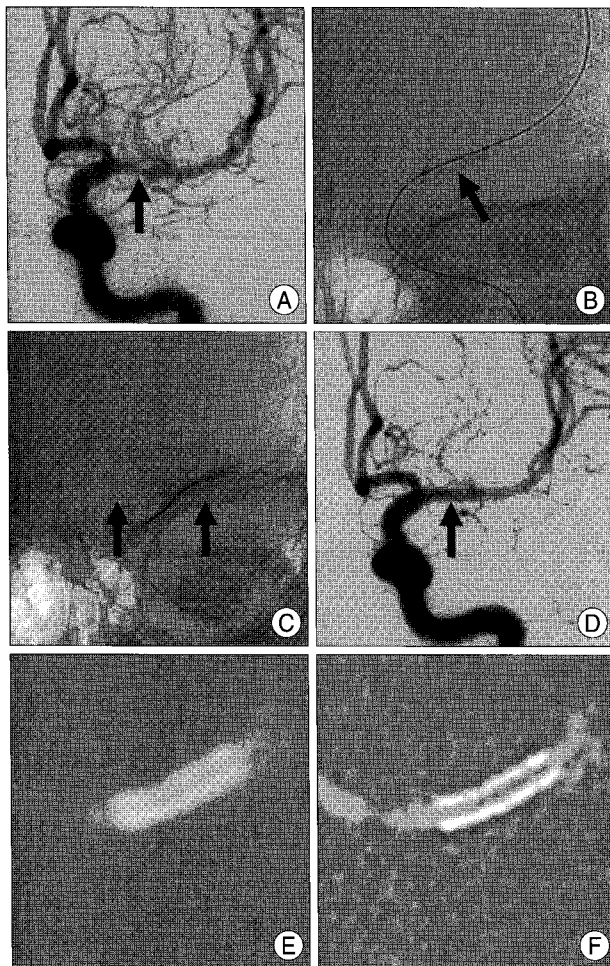


**Fig. 3.** A 56-year-old female presented with headache and recurrent TIA of right hemiparesis. A : Anteroposterior view of the left internal carotid artery (ICA) angiogram shows diffuse severe stenosis (arrow, about 85%) on the M1 portion of the left MCA correlating with recurrent TIA symptoms. B and C : Anteroposterior radiographs show the stent (arrows) during and after deployment in the M1 portion. The used stent is a 2.5/12 mm-sized coronary stent (Flexmaster, JoMed). D : On the post-procedural anteroposterior radiograph and angiogram, the MCA has a smooth appearance, normalized diameter of the lumen, and preservation of the lenticulostriate arteries (arrow). E : Computed tomography angiography with 16 MSCT is performed at the 2nd post-stenting days. Curved axial multiplanar reconstruction with standard sharp kernel (H30f) shows about 37% lumen visibility on the M1 portion of the left MCA. F : Curved axial multiplanar reconstruction with optimized sharp kernel (H60f) shows about 57% lumen visibility on the M1 portion of the left MCA.

cranial ICA and vertebrobasilar artery (VBA) stenosis<sup>14,15</sup>.

The method of choice for the detection of restenoses within stented cerebral vessel segment is intra-arterial catheter angiography, a method that is associated with an incidence of neurological complications in about 0.5-1.3% of the patients<sup>4,19,20</sup> and an incidence of clinically silent brain lesions in about 20% of the patients<sup>1</sup>. Recent *in-vitro* studies have shown that CT angiographic evaluation of small vessel patency after stenting is possible but considerably impaired by artificial lumen narrowing due to artifacts

from the stents struts<sup>5</sup>.

In previous experimental study on coronary artery stent<sup>13</sup> demonstrated an improvement of stent lumen visualization and in-stent stenosis detection for 16-slice CT and the improvement was highly significant using the new dedicated sharp coronary reconstruction kernel on a 16-slice CT. The convolution kernel had the most significant influence on the visibility of the lumen of individual stents<sup>11</sup>. Although CT coronary angiography is typically performed using a medium smooth convolution kernel (B30f), a dedicated convolution kernel (B46f) for visualization of coronary stents was developed<sup>16</sup>. In this kernel, the modulation transfer function was optimized to reduce blurring that typically occurs close to borders with high attenuation differences. This effect resulted in a sharper delineation of each stent. The stent lumen was more clearly depicted and the attenuation values within the stent lumen significantly less altered<sup>11</sup>. Another factor with major influence on stent visualization was the scanner hardware. The 16- detector row MSCT scanner with sub-millimeter collimation proved superior when compared with the 4-detector row MSCT scanner with  $4 \times 1$  mm collimation. The effective slice thickness calculated from the data of the 4-detector row MSCT scanner was 25% thicker when compared with the data from the 16-detector row MSCT scanner<sup>11</sup>.

In our study, we used H60f kernel as the dedicated optimized sharp kernel for better visualization of intracranial stent lumen and this kernel is almost similar to B60f kernel for optimized coronary stent. Our result of lumen visualization for intracranial stent is superior to those for coronary stent and may be because intracranial arteries, such as middle cranial artery, petrocavernous portion of internal carotid artery, intracranial vertebral artery are less movable than coronary artery and the dedicated optimized sharp kernel could reduce an exaggerated thickening or blooming of the stent struts, resulting in artificial lumen narrowing of the stented tubes. Previous *in vitro* study<sup>13</sup>, using the new dedicated sharp coronary reconstruction kernel on a 16-slice CT, attenuation value of the stent lumen was similar to the unstented vessel part (250 HU). In our *in vivo* study, however, difference of attenuation value between stent lumen and unstented vessel lumen was statistically significant ( $p < 0.05$ ). The average range of attenuation value of lumen was about 212-215 HU and those of proximal unstented lumen being about 310-318. Although these differences may be regarded as artifact by beam hardening, further study should be needed for proof of meaning of these differences, such as difference related with in-stent restenoses in intracranial stents.

16-slice MSCT angiography may be a useful, noninvasive modality for evaluation of intracranial stents patency. CT angiography, however, has limitations on the exact assessment of in-stent lumen including residual stenosis and restenosis because of its artifacts, partial volume effects, and low spatial resolution compared with invasive angiography, especially in cases of presence with calcified plaque. Further study on these limitations should be followed with recently developed more 64 slice MSCT.

## CONCLUSION

In conclusion, 16-slice CT using the dedicated sharp kernel for assessment of intracranial stent (H60f) may provide a useful information for evaluation of patency of stent and lumen diameter of intracranial stents.

## References

- Bendszus M, Koltzenburg M, Burger R, Warmuth-Metz M, Hofmann E, Solymosi L : Silent embolism in diagnostic cerebral angiography and neurointerventional procedures : a prospective study. *Lancet* 354 : 1594-1597, 1999
- Betriu A, Masotti M, Serra A, Alonso J, Fernández-Avilés F, Gimeno F, et al : Randomized comparison of coronary stent implantation and balloon angioplasty in the treatment of de novo coronary artery lesions (START) : a four-year follow-up. *J Am Coll Cardiol* 34 : 1498-1506, 1999
- Gomez CR, Misra VK, Campbell MS, Soto RD : Elective stenting of symptomatic middle cerebral artery stenosis. *AJNR* 21 : 971-973, 2000
- Grzyska U, Freitag J, Zeumer H : Selective cerebral intraarterial DSA. Complication rate and control of risk factors. *Neuroradiology* 32 : 296-299, 1990
- Hahnel S, Trossbach M, Braun C, Heiland S, Knauth M, Sartor K, et al : Small-vessel stents for intracranial angioplasty : in vitro comparison of different stent designs and sizes by using CT angiography. *AJNR* 24 : 1512-1516, 2003
- Karas SP, Gravanis MB, Santoian EC, Robinson KA, Anderberg KA, King SB 3rd : Coronary intimal proliferation after balloon injury and stenting in swine : an animal model of restenosis. *J Am Coll Cardiol* 20 : 467-474, 1992
- Lederman RJ, Mendelsohn FO, Santos R, Phillips HR, Stack RS, Crowley JJ : Primary renal artery stenting : characteristics and outcomes after 363 procedures. *Am Heart J* 142 : 314-323, 2001
- Lee TH, Kim DH, Lee BH, Kim HJ, Choi CH, Park KP, et al : Preliminary results of endovascular stent-assisted angioplasty for symptomatic middle cerebral artery stenosis. *AJNR* 26 : 166-174, 2005
- Levy EI, Hanel RA, Bendok BR, Boulos AS, Hartney ML, Guterman LR, et al : Staged stent-assisted angioplasty for symptomatic intracranial vertebrobasilar artery stenosis. *J Neurosurg* 97 : 1294-1301, 2002
- Lylyk P, Cohen JE, Ceratto R, Ferrario A, Miranda C : Angioplasty and stent placement in intracranial atherosclerotic stenoses and dissections. *AJNR* 23 : 430-436, 2002
- Mahnken AH, Buecker A, Wildberger JE, Ruebben A, Stanzel S, Vogt F, et al : Coronary artery stents in multislice computed tomography : in vitro artifact evaluation. *Invest Radiol* 39 : 27-33, 2004
- Maintz D, Grude M, Fallenberg EM, Heindel W, Fischbach R : Assessment of coronary arterial stents by multislice-CT angiography. *Acta Radiol* 44 : 597-603, 2003
- Maintz D, Seifarth H, Flohr T, Krämer S, Wichter T, Heindel W, et al : Improved coronary artery stent visualization and in-stent stenosis detection using 16-slice computed-tomography and dedicated image reconstruction technique. *Invest Radiol* 38 : 790-795, 2003
- Mori T, Kazita K, Chokyu K, Mima T, Mori K : Short-term arteriographic and clinical outcome after cerebral angioplasty and stenting for intracranial vertebrobasilar and carotid atherosclerotic occlusive disease. *AJNR* 21 : 249-254, 2000
- Nakahara T, Sakamoto S, Hamasaki O, Sakoda K : Stent-assisted angioplasty for intracranial atherosclerosis. *Neuroradiology* 44 : 706-710, 2002
- Siemens Inc. Somatom 16 application Guide : Special Protocols. *Forchheim* : 28-31, 2002
- Shin YS, Kim SY, Bang OY, Jeon P, Yoon SH, Cho KH, et al : Early experiences of elective stenting for symptomatic stenosis of the M1 segment of the middle cerebral artery : reports of three cases and review of the literature. *J Clin Neurosci* 10 : 53-59, 2003
- Trossbach M, Hartmann M, Braun C, Sartor K, Hahnel S : Small vessel stents for intracranial angioplasty : in vitro evaluation of in-stent stenoses using CT angiography. *Neuroradiology* 46 : 459-463, 2004
- Waugh JR, Sacharias N : Arteriographic complications in the DSA era. *Radiology* 182 : 243-246, 1992
- Willinsky RA, Taylor SM, TerBrugge K, Farb RI, Tomlinson G, Montanera W : Neurologic complications of cerebral angiography : prospective analysis of 2,899 procedures and review of the literature. *Radiology* 227 : 522-528, 2003
- Yadav JS, Roubin GS, Iyer S, Vitek J, King P, Jordon WD, et al : Elective stenting of the extracranial carotid arteries. *Circulation* 95 : 376-381, 1997